MATERIALS CHEMISTRY FRONTIERS

RESEARCH ARTICLE

View Article Online
View Journal | View Issue

Check for updates

Cite this: *Mater. Chem. Front.*, 2020, **4**, 3616

A new family of liquid and solid guanidine-based n-type dopants for solution-processed perovskite solar cells†

Hidenori Nakayama, [abc] Julia A. Schneider, [bcd] Mina Faust,[b] Hengbin Wang, [c] Javier Read de Alaniz [bc] and Michael L. Chabinyc *[bc]

Received 1st July 2020,
Accepted 27th July 2020

DOI: 10.1039/d0qm00437e

rsc.li/frontiers-materials

We present a series of new dopants based on a bicyclcic guanidine-type structure, 1,5,7-triazabicyclo[4.4.0]dec-5-ene (**TBD**), for organic semiconductors. A series of **TBD** derivatives that were alkylated at the 7-position were synthesized and their physical properties were determined. These stable dopants were shown to be effective n-type dopants for [6,6]-phenyl-C_{61}-butyric acid methyl ester ($PC_{61}BM$), poly{[*N*,*N*′-bis(2-octyldodecyl)naphthalene-1,4,5,8-bis(dicarboximide)-2,6-diyl]-*alt*-5,5′-(2,2′-bithiophene)} (P(NDI2OD-T2)) and 3,9-bis(2-methylene-(3-(1,1-dicyanomethylene)-indanone))-5,5,11,11-tetrakis(4-hexylphenyl)-dithieno[2,3-*d*:2′,3′-*d*′]-*s*-indaceno[1,2-*b*:5,6-*b*′]dithiophene (ITIC). Films of $PC_{61}BM$ doped with 10 mol% of a dimeric derivative of **TBD** had electrical conductivities of 0.065 S cm^{-1}. The utility of the dopants was further shown by doping electron transport layers of $PC_{61}BM$ with **2TBD-C10** for methyl ammonium lead iodide ($MAPbI_3$) solar cells leading to improved fill factors and PCEs relative to undoped ETLs.

Published on 27 juli 2020. Downloaded on 03.08.2025 1:40:23.

Introduction

The use of organic semiconductors in applications, such as solar cells, light-emitting diodes, field-effect transistors, and thermoelectric devices, presents a need for efficient dopants.[1–3] Electrical doping of organic semiconductors is necessary to control their conductivity, fill electronic trap states, and to modify carrier-injection barriers at interfaces by shifting line-up of transport levels. Particularly sought after are n-type dopants for transport layers in solar cells and light emitting diodes. While n-type dopants with low ionization potentials, *e.g.* tetrathiafulvalene (TTF),[4,5] can be used with a wide variety of organic semiconductors they are not stable under ambient conditions due to their low oxidation potentials. In addition, the dopant must also be incorporated into the semiconductor uniformly which is particularly important for transport layers in solar cells.

A number of strategies have been used to develop air-stable n-type dopants. Latent species have been used by generating the reductive species *in situ* from a stable precursor, for example the hydride-donor leuco crystal violet (LCV) is generated from the crystal violet salt and benzimidazoline radicals.[6] Other strategies include the use of weak bonds that allow cleavage coupled with electron transfer, *e.g.* a dimer of the 2,3-dihydro-1*H*-benzimidazole $(2\text{-Cyc-DMBI})_2$,[7] or photoactivation of the electron transfer raction.[8] Organometallic species have been designed such that they may be stable in their undoped form or leverage the latent dopant strategy.[3,9,10]

Tertiary amines have been explored as n-type dopants.[11–14] Tetrakis(dimethylamino)ethylene (TDAE) is a strong reducing agent and has been used to n-type dope organic semiconductors or to compensate for p-type doping.[15] A drawback of TDAE is its volatility, but appropriate functionalization to increase its mass has led to effective n-type doping while still maintaining its solubility.[16] The electron transfer reactions of cyclic amines such as diazabicyclo(5.3.0)non-5-ene (DBN) and 1,8-diazabicyclo(5.4.0)undec-7-ene (DBU) with C_{60} have also been examined.[17,18] DBU was found to react with C_{60} by electron transfer to form the radical ions C_{60}^- and DBU^+, followed by formation of a diamagnetic adduct with and optical absorbance in the near infrared region.[17] Recently addition of DBU was found to lead to increases in the electrical conductivity of [6,6]-phenyl-C_{61}-butyric acid methyl ester ($PC_{61}BM$), poly{[*N*,*N*′-bis(2-octyldodecyl)naphthalene-1,4,5,8-bis(dicarboximide)-2,6-diyl]-*alt*-5,5′-(2,2′-bithiophene)} (P(NDI2OD-T2)) and 3,9-bis(2-methylene-(3-(1,1-dicyanomethylene)-indanone))-5,5,11,11-tetrakis(4-hexylphenyl)-dithieno[2,3-*d*:2′,3′-*d*′]-*s*-indaceno[1,2-*b*:5,6-*b*′]

[a] *Electronics Materials and New Energy Laboratory, Mitsubishi Chemical Corporation, Yokohama R&D Center 1000, Kamoshida-cho, Aoba-ku, Yokohama 227-8502, Japan*
[b] *Materials Department, University of California, Santa Barbara, California 93106, USA. E-mail: mchabinyc@engineering.ucsb.edu*
[c] *Mitsubishi Chemical Center for Advanced Materials, University of California, Santa Barbara, California 93106, USA*
[d] *Department of Chemistry, Fordham University, Bronx, New York 10458, USA*

† Electronic supplementary information (ESI) available. See DOI: 10.1039/d0qm00437e

 This journal is © The Royal Society of Chemistry and the Chinese Chemical Society 2020

Published on 27 juli 2020. Downloaded on 03.08.2025 1:40:23.

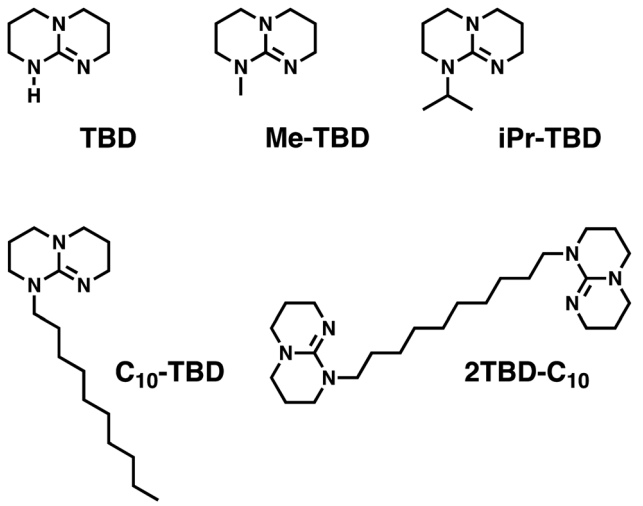

Fig. 1 The chemical structures of n-dopants based on 1,5,7-triazabicyclo [4.4.0]dec-5-ene (**TBD**).

dithiophene (ITIC).[19] Electron spin resonance (ESR) demonstrated the formation of radical species in each case, but the mechanism of doping and whether adducts were formed were not explored. Similarly 1-(*o*-tolyl) biguanide was found to dope $PC_{61}BM$ and used as an electron transport layer in MAPbI3 solar cells.[20] For many tertiary amines, like DBU, their oxidation potential is such that the electron transfer reaction with many organic semiconductors is not thermodynamically favorable and either close contact of the resulting charge separated species or a subsequent reaction makes the doping process favorable.

Herein, we present a series of new triazabicyclodecene-based n-dopants with varying physical properties, namely **TBD**, **iPr-TBD**, **Me-TBD**, **C10-TBD**, **2TBD-C10** (Fig. 1). **TBD** is a well-known catalyst for transesterification and is considered a superbase.[21,22] We are not aware of its use as a dopant for organic semiconductors. The chemistry of **TBD** allows for simple substitution at the nitrogen atom in the 7-position allowing for control of its volatility and physical state at room temperature. There have been relatively few reports of a systematic variation of the structure of n-type dopants for organic semiconductors.[3,7,23,24] We therefore examined the impact of this functionalization on the performance as dopants in several organic semiconductors including $PC_{61}BM$, P(NDI2OD-T2) and ITIC. Their utility was further shown by doping electron transport layers of $PC_{61}BM$ with **2TBD-C10** in methyl ammonium lead iodide ($MAPbI_3$) solar cells leading to improved fill factors and PCEs relative to undoped ETLs.

Results and discussion

Design and synthesis of TBD-based dopants

We based our investigation of n-type dopants around bicyclic guanidine derivatives (Fig. 1). The parent compound is 1,5,7-triazabicyclo[4.4.0]dec-5-ene (**TBD**), which is considered a superbase because of its high Brønsted basicity. The three nitrogen atoms around the central carbon atom provide three equivalent resonance structures, sometimes referred to as Y-aromaticity because of the cross conjugation through a central atom.[25,26] By introducing alkyl substituents on **TBD**, we can alter its physical characteristics and its reactivity, hindering possible side reactions such as nucleophilic substitution with organic semiconductors.

7-Methyl-1,5,7-triazabicyclo[4.4.0]dec-5-ene (**Me-TBD**) was commercially available and used without further purification. **TBD** was readily alkylated with primary and secondary alkyl halides by deprotonating with sodium hydride and quenching with the alkyl bromide to yield **iPr-TBD**, **C10-TBD**, and **2TBD-C10**. In contrast, we found that tertiary alkyl halides were not reactive under the conditions used. Details of the synthetic procedure are given in the ESI,† and NMR spectra of the compounds are given in Fig. S1–S3 (ESI†). **TBD** is a crystalline white solid, but **Me-TBD**, **iPr-TBD**, and **C10-TBD** are oils, with **iPr-TBD** being by far the most viscous. **2TBD-C10** is a white powdery solid likely due to the presence of two **TBD** units per molecule. All of the derivatives are readily soluble in both polar and non-polar organic solvents, as well as water and methanol. This allows for versatile processing, employing either blends or sequential applications with anti-solvents. As well, this dopant family can be isolated and purified in non-anhydrous solvents and stored in air.

The structure of **TBD** bearing three external nitrogen atoms provides the potential for constructing quaternary ammonium salts *via* *N*-alkylation of the tertiary amines. As such, our reaction conditions were designed to minimize this possibility by keeping **TBD** in excess relative to the alkyl halide whenever feasible. The reaction of **TBD** with 1,4-dibromobutane was a notable exception that led exclusively to an intramolecular cyclization yielding a **TBD** derivative with a fused 7-membered ring (see ESI,† and Fig. S4). With shorter chains it appears the proximity of the secondary alkyl bromide to the Schiff base nitrogen facilitates intramolecular cyclization over the reaction with a second equivalent of **TBD**. As the resulting cyclic product with 1,4-dibromobutane is already cationic it was eliminated from our studies.

Our principle motivation behind modifying commercially available **TBD** was to enhance the stability of the dopant during processing. The volatility of dopants can drastically alter their concentration in thin films after coating and thermal annealing. To this end, we quantified the thermal stability of our dopants through thermal gravimetric analysis (TGA) (Fig. S5, ESI†). We found that modifying **TBD** with short alkyl chains, especially branched isopropyl groups, led to much lower initial decomposition temperatures. Longer alkyl chains like decyl, on the other hand, increased the thermal stability. **2TBD-C10**, a solid like **TBD**, but with the added mass of the decyl chain, showed the highest thermal stability, with an initial decomposition temperature around 270 °C.

Electronic properties

In order to act as efficient n-dopants, the **TBD** moiety must be readily oxidized to allow electron transfer to the organic semiconductor. Density functional theory (DFT) calculations show the highest occupied molecular orbital (HOMO) of Me-TBD

Published on 27 juli 2020. Downloaded on 03.08.2025 1:40:23.

having contributions from the nitrogen atoms with a node at their central carbon atom as expected (Fig. S6, ESI†). We expect the series to behave similarly due to the simple alkyl substitution and used cyclic voltammetry (CV) to compare the oxidation potentials of **C10-TBD** and **2TBD-C10** (Fig. S7, ESI†). Both dopants showed highly irreversible oxidation potentials near ≈1.0 V relative to a ferrocene/ferrocenium (Fc/Fc^+) reference. This close match suggests that the two tethered **TBD** moieties in **2TBD-C10** behave independently. The oxidation potential from CV represents an ionization energy (HOMO level) of about 5.1 eV for both dopants that is intermediate between other comparable tertiary amine dopants. TDAE is a strong reducing agent with an oxidation potential of ≈−1 V *vs.* Fc/Fc^+.[27,28] The oxidation potential of DBU has not been reported in studies of its use as a dopant, but it is a weaker reducing agent than TDAE.[19] We used DFT to calculate the difference in gas-phase ionization energy between TBD-Me and DBU and find that TBD-Me is 0.45 eV easier to ionize. The **TBD** series should therefore provide improved stability in ambient relative to TDAE and a higher driving force for electron transfer than DBU.

n-Type doping of organic semiconductors

We compared the performance of the new **TBD**-based dopants to DBU as a dopant for $PC_{61}BM$. $PC_{61}BM$ is a key material other as a component in organic solar cells[29] and as an electron transport layers in other applications.[15] The in-plane electrical conductivities of doped $PC_{61}BM$ films indicate that **2TBD-C10** gives the best conductivity of the series of dopants and gives higher performance than DBU (Fig. 2 and Table S1, ESI†). The dopants were added over a range of doping ratios, 0.1 to 10 mol% and a super-linear relationship was found between the electrical conductivity and doping ratio (Fig. 2). The data fits well to a simple power law ($y = y_0 + Ax^{\alpha}$) with α of ≈1.3; super-linear behavior is a common feature of hopping conduction in molecular semiconductors.[30] It is notable that the electrical conductivity of $PC_{61}BM$ films doped with **2TBD-C10** (6.5×10^{-2} S cm^{-1}) is as high as that of films doped with $(2\text{-Cyc-DMBI})_2$: the maximum conductivity of $(2\text{-Cyc-DMBI})_2$ doped $PC_{61}BM$ films is reported to be 4.7×10^{-3} S cm^{-1} at 10 mol% addition.[7] If each dopant led to the formation of 1 charge carrier, then the electron mobility can be estimated as ≈4×10^{-3} cm^2 V^{-1} s^{-1} at 10 mol% and ≈1×10^{-2} cm^2 V^{-1} s^{-1} at 1 mol% based on a mass density of $PC_{61}BM$ of ≈1.5 g cm^{-3}. These values are comparable to mobilities of ≈4×10^{-2} cm^2 V^{-1} s^{-1} extracted from the current–voltage characteristics of thin film transistors of $PC_{61}BM$ doped with ~1 mol% of N-DMBI.[31] While it is difficult to quantitatively extract the efficiency of doping, it must be relatively high otherwise the carrier mobility would need to be larger than typically observed to account for the electrical conductivity. The effectiveness of **2TBD-C10** as a dopant can partly be explained by its good miscibility with $PC_{61}BM$. The AFM topography images of doped $PC_{61}BM$ films show no aggregation or phase separation for each concentration and look similar to that of a pristine PCBM film (Fig. S8, ESI†).

We find that the alkylation of the 7-position of **TBD** affects both the electrical conductivity and processability of doped

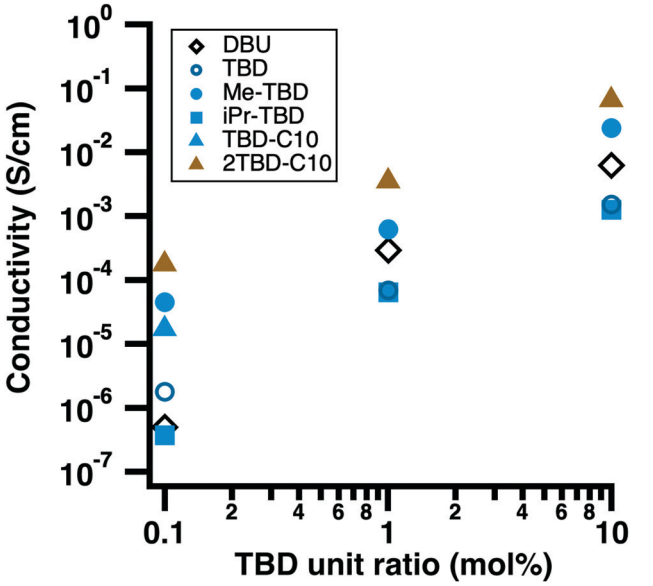

Fig. 2 Electrical conductivities of films of $PC_{61}BM$ doped with **TBD**-derivatives and DBU as a function of the molar ratio. **TBD-C10** has a data point only at 0.1 mol% because films could not be cast at higher molar ratios.

films of $PC_{61}BM$. The branched isopropyl derivative, **iPr-TBD**, gave similar electrical conductivities as **TBD** suggesting that the alkylation itself is not the sole origin of the increase. The addition of relatively long linear alkyl groups, *i.e.* **TBD-C10**, led difficulties in casting doped films at high molar ratios due to dewetting of the films from the substrate. We attribute this issue to the surfactant-like nature of its structure of **TBD-C10**. This issue was eliminated by using the dimer, **2TBD-C10**, which was processable at all concentration used.

$PC_{61}BM$ films doped by **2TBD-C10** are more tolerant to thermal annealing than those by **TBD**s with short side chains. The conductivity of 1 mol% **2TBD-C10** doped PCBM film increased from 3.5×10^{-3} to 7.4×10^{-3} S cm^{-1} after thermal annealing on a hot plate in nitrogen at 150 °C for 30 min, whereas that of **Me-TBD** doped one dropped from 6.2×10^{-4} to 5.6×10^{-5} S cm^{-1} in the same treatment. This change is well-correlated to the TGA data for the dopants that showed a higher decompositions temperature for longer chain derivatives. The improved processability of **2BD-C10** and its higher tolerance to thermal treatments led us to focus on this dopant relative to others in the series.

We measured grazing incident wide angle X-ray scattering (GIWAXS) to determine if there were signs of aggregation or changes in the structural order of doped $PC_{61}BM$ thin films. The scattering patterns of $PC_{61}BM$ films without dopant and with 10 mol% of **2TBD-C10**, **Me-TBD**, and **iPr-TBD** are almost identical (Fig. 3 and Fig. S9, ESI†). They have two rings at around q = 0.7 and 1.4 Å^{-1} with full width at half maximum (FWHM) of about 0.20 and 0.15 Å^{-1}, respectively, indicating those films are amorphous as typically seen in fullerene films. We found that the peaks shift slightly toward lower q range by ≈0.03 Å^{-1} upon doping, which is a small shift given the FWHM of the peaks. Importantly, we do not observe any new peaks

 This journal is © The Royal Society of Chemistry and the Chinese Chemical Society 2020

Published on 27 juli 2020. Downloaded on 03.08.2025 1:40:23.

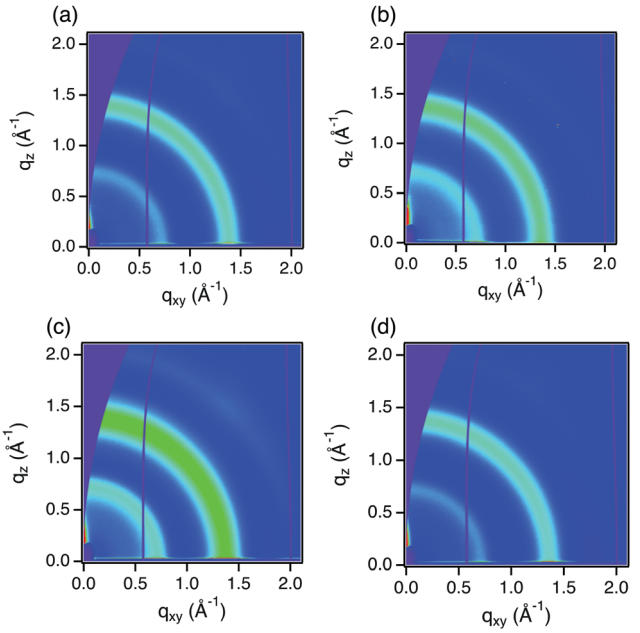

Fig. 3 2-Dimensional GIWAXS images of (a) pristine $PC_{61}BM$, (b) $PC_{61}BM$ with 10 mol% **2TBD-C10**, (c) $PC_{61}BM$ with 10 mol% **Me-TBD**, and (d) $PC_{61}BM$ with 10 mol% **iPr-TBD**.

upon doping with **2TBD-C10**, a solid dopant suggesting that there are no aggregates of the dopant and likely molecularly mixing of the compound with $PC_{61}BM$. If an adduct is formed between the dopant and $PC_{61}BM$, it does not strongly perturb the structure of doped $PC_{61}BM$ films relative to undoped films.

We found that addition of **2TBD-C10** leads to n-type doping of organic semiconductors beyond $PC_{61}BM$. We examined the doping of P(NDI2OD-T2), a well-studied naphthalenediimide based conjugated polymer, because it has been broadly used as a test case for n-type doping and it has an electron affinity near that of $PC_{61}BM$.[7,9,19,24,28] Thin films of P(NDI2OD-T2) doped with **2TBD-C10** at 10 mol% have an electrical conductivity of 7.0×10^{-4} S cm^{-1} (Table 1). This value is comparable to value using $(2\text{-Cyc-DMBI})_2$ (2.8×10^{-3} S cm^{-1} with 11 mol%)[7] and N-DMBI (8×10^{-4} S cm^{-1} with 10 mol%)[24] as dopants. In contrast, **TBD-C10** gives three orders of magnitude lower conductivity (1.5×10^{7} S cm^{-1}) in 10 mol% doping, indicating that the dimer is significantly more effective. **2TBD-C10** also dopes ITIC, an accepter–donor–acceptor shape non-fullerene acceptor for organic photovoltaics, yielding conductivities of 4.3×10^{-6} and 1.7×10^{-6} S cm^{-1} with 10 and 1 mol% doping, respectively. These relatively low conductivities are partly due to lower electron mobility in ITIC ($\sim 10^{-2}$ cm^2 V^{-1} s^{-1}) than that of $PC_{61}BM$ ($\sim 10^{-1}$ cm^2 V^{-1} s^{-1}) based on measurements of field-effect transistors.[32]

The scattering patterns of P(NDI2OD-T2) are also insensitive to doping with **2TBD-C10** and **TBD-C10** (Fig. 4 and Fig. S10 ESI†). The scattering pattern of pristine P(NDI2OD-T2) show a π-staking feature at 1.6 Å^{-1} in the out-of-plain direction and alkyl stacking features at 0.25 and 0.47 Å^{-1} in the in-plane direction, indicating a face-on orientation of its crystalline moieties. Addition of **2TBD-10** or **TBD-C10** does not result in

Table 1 Electrical conductivities (S cm^{-1}) of thin films of organic semiconductors as a function of concentration of the TBD dopant

	2TBD-C10	**2TBD-C10**	**2TBD-C10**	**TBD-C10**
Dopant concentration	10 mol%	1 mol%	0.1 mol%	10 mol%
$PC_{61}BM$	6.5×10^{-2}	3.5×10^{-3}	1.8×10^{-4}	nd[b]
P(NDI2OD-2T)	7.0×10^{-4}	2.4×10^{-6}	nd[a]	1.5×10^{-7}
ITIC	4.3×10^{-6}	1.7×10^{-6}	nd[a]	nd[b]

[a] Too low to measure. [b] The films were not obtained due to dewetting.

notable shift of the polymer originated peaks or appearance of new peaks. We thus conclude that the crystalline domains of the polymer are impenetrable to these **TBD** dopants, and the dopants reside in the amorphous regions. This conclusion is not unique to the **TBD** dopants and also holds true for conventional dopants such as N-DMBI as we previously reported.[5]

Doping electron transport layers in perovskite solar cells

Doping of the hole and electron transport layers in organic metal halide (perovskite) solar cells has proven to be a beneficially strategy for improving their performance.[33–37] Organic amines have been used to improve carrier extraction in organic electron transport layers (ETLs) of perovskite solar cells. Polyethyleneimine (PEIE) has frequently been used as an interlayer to modify the work function at electrodes by doping or forming interfacial dipole layers.[38,39] Poly[(9,9-bis(3′-(*N*,*N*-dimethylamino) propyl)-2,7-fluorene)-*alt*-2,7-(9,9-dioctylfluorene)] (PFN) has been used as an effective interlayer with $PC_{61}BM$ ETLs in perovskite solar cells,[40] with some attributing the improvement due to doping.[37] Co-polymers of PFN and napthalenediimides as ETLs have also shown to lead to good fill factors in solar cells as well

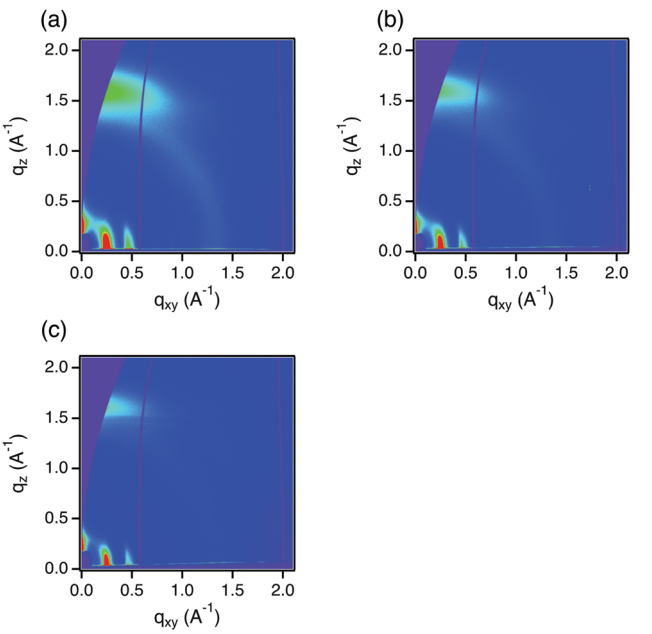

Fig. 4 2-Dimensional GIWAXS scattering of (a) pristine P(NDI2OD-T2), (b) P(NDI2OD-T2) with 10 mol% **2TBD-C10**, and (c) P(NDI2OD-T2) with 10 mol% **TBD-C10**.

Published on 27 juli 2020. Downloaded on 03.08.2025 1:40:23.

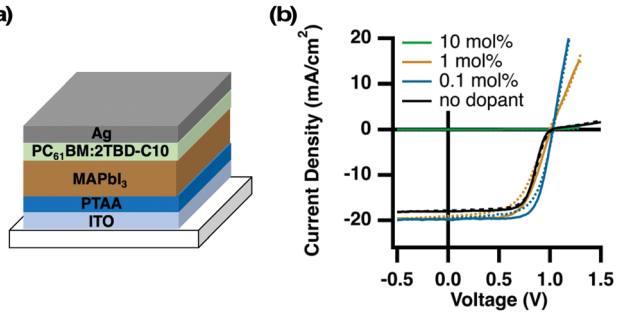

Fig. 5 (a) Schematic of the solar cell structure of glass/ITO (20 Ω sq^{-1})/polytriarylamine (PTAA, ~5 nm)/$MAPbI_3$ (~400 nm)/$PC_{61}BM$:dopant (~100 nm)/Ag (80 nm) (b) *J–V* characteristics of $MAPbI_3$ photovoltaics using $PC_{61}BM$ doped with **2TBD-C10** in a ratio of (black) 0 mol%, (blue) 0.1 mol%, (gold) 1 mol% and (green) 10 mol%. Dashed lines represent forward scans, while solid lines reverse scans.

demonstrating the broad utility of aliphatic tertiary amine functionalities.[41] The success of these materials suggested that the **TBD**-dopants would be compatible with perovskite solar cells.

To demonstrate the utility of the **TBD**-based dopants, we fabricated solar cells of methylammonium lead triiodide ($MAPbI_3$) with an inverted structure, *i.e.* ETL cast on top of the $MAPbI_3$ layer (Fig. 5). We examined **2TBD-C10** doped $PC_{61}BM$ as the ETL to assess the impact of doping on the behavior of the solar cells. The device stack is glass/ITO (20 Ω sq^{-1})/polytriarylamine (PTAA, ~5 nm)/$MAPbI_3$ (~400 nm)/$PC_{61}BM$ (~100 nm)/Ag (80 nm). The results clearly show that doping $PC_{61}BM$ with **2TBD-C10** works to improves the performance with a clear optimal molar ratio of dopant (Table 2 and Fig. 5). The devices without doping give a power conversion efficiency (PCE) of 11.8% with kink in the current–voltage (*J–V*) characteristic around the V_{OC} condition (J = 0 mA cm^{-2}). Because the J_{SC} (18.0 mA cm^{-2}) of the solar cell is reasonable given the thickness of the $MAPbI_3$ layer, the kink is a sign of an electron injection barrier at the Ag/$PC_{61}BM$ interface due to Schottky barrier formation. When $PC_{61}BM$ is doped with 0.1 mol% of **2TBD-C10**, the kink disappears giving a PCE of 14.5% with improved fill-factor (FF) of 0.71. Further addition of the dopant, however, leads to deterioration of the device performance. With 1 mol% of doping, FF is reduced to 0.61 while retaining the V_{OC} and J_{SC}, giving a PCE of 12.3%. With 10 mol%, the J_{SC} is almost entirely quenched and the solar cell has very poor performance. We previously found that increase the doping of ETLs can lead to decomposition of the surface of $MAPbI_3$ by inducing release of iodine.[42] It is possible that similar degradation happens here in the highly doped devices, increasing the resistance at the $MAPbI_3$/$PC_{61}BM$ interface and blocking charge extraction from the bulk of the active layer.

Table 2 Device parameters of $MAPbI_3$ based photovoltaics with the structure: glass/ITO/PTAA/$MAPbI_3$/$PC_{61}BM$:2TBD-C10/Ag

2TBD-C10 (mol%)	V_{OC} (V)	J_{SC} (mA cm^{-2})	FF	PCE (%)
0 (not doped)	1.02 ± 0.00	18.0 ± 0.33	0.64 ± 0.01	11.8 ± 0.5
0.1	1.02 ± 0.00	19.8 ± 0.15	0.70 ± 0.01	14.4 ± 0.17
1	1.00 ± 0.02	19.2 ± 0.45	0.60 ± 0.02	11.7 ± 0.68
10	~0.2	<0.01	~0.2	<0.1

Conclusions

In conclusion, we have shown that triazabicylodecene-based compounds can effectively dope n-type organic semiconductors, including $PC_{61}BM$. Tethering two **TBD** moieties with a simple alkyl chain gave a solid dopant, **2TBD-C10**, with high thermal stability above 250 °C and effective doping of a range of organic semiconductors. $PC_{61}BM$ films doped by **2TBD-C10** were the most tolerant to thermal annealing and reached in-plane conductivities of 6.5 × 10^{-2} S cm^{-1}. Furthermore, using $PC_{61}BM$ doped with **2TBD-C10** as the electron transport layer (ETL) in $MAPbI_3$ photovoltaics led to a 23% increase in performance, from 11.8% to 14.5% PCE. Although beyond the scope of this report, there may be added benefits of using superbases like the **TBD** series as n-type dopants with perovskite solar cells. The ability of **TBD** and its conjugate Lewis acid to complex, or react, with stray metal atoms,[43,44] CO_2,[45,46] and reactive oxygen species[47,48] could further improve the stability of devices.

Conflicts of interest

A patent has been filed by the authors on the use of **TBD**-derivatives as dopants.

Acknowledgements

Work on the mechanism of doping was supported by NSF DMR 1808622. Portions of the research were carried out at the Advanced Light Source, supported by the Director, Office of Science, Office of Basic Energy Sciences, of the U.S. Department of Energy under Contract No. DEAC02-05CH11231. The research reported here made use of shared facilities of the UCSB MRSEC (NSF DMR 1720256), a member of the Materials Research Facilities Network (www.mrfn.org). Use was made of computational facilities purchased with funds from the National Science Foundation (CNS-1725797) and administered by the Center for Scientific Computing (CSC). The CSC is supported by the California NanoSystems Institute and the Materials Research Science and Engineering Center (MRSEC; NSF DMR 1720256) at UC Santa Barbara. The authors thank Prof. Fred Wudl (UCSB) for many helpful discussions on this work and for his many pioneering contributions to the field of materials chemistry.

References

1 B. Lüssem, C.-M. Keum, D. Kasemann, B. Naab, Z. Bao and K. Leo, Doped Organic Transistors, *Chem. Rev.*, 2016, **116**, 13714–13751.
2 B. Russ, A. Glaudell, J. J. Urban, M. L. Chabinyc and R. A. Segalman, Organic thermoelectric materials for energy harvesting and temperature control, *Nat. Rev. Mater.*, 2016, **1**, 1–14.

 This journal is © The Royal Society of Chemistry and the Chinese Chemical Society 2020

Published on 27 juli 2020. Downloaded on 03.08.2025 1:40:23.

3 S. Guo, S. B. Kim, S. K. Mohapatra, Y. Qi, T. Sajoto, A. Kahn, S. R. Marder and S. Barlow, n-Doping of Organic Electronic Materials using Air-Stable Organometallics, *Adv. Mater.*, 2012, **24**, 699–703.
4 F. Wudl, G. M. Smith and E. J. Hufnagel, Bis-1,3-dithiolium chloride: an unusually stable organic radical cation, *J. Chem. Soc., Chem. Commun.*, 1970, 1453.
5 M. Bendikov, F. Wudl and D. F. Perepichka, Tetrathiafulvalenes, Oligoacenenes, and Their Buckminsterfullerene Derivatives: The Brick and Mortar of Organic Electronics, *Chem. Rev.*, 2004, **104**, 4891–4946.
6 F. Li, A. Werner, M. Pfeiffer, K. Leo and X. Liu, Leuco Crystal Violet as a Dopant for n-Doping of Organic Thin Films of Fullerene C $_{60}$, *J. Phys. Chem. B*, 2004, **108**, 17076–17082.
7 B. D. Naab, S. Zhang, K. Vandewal, A. Salleo, S. Barlow, S. R. Marder and Z. Bao, Effective Solution- and Vacuum-Processed n-Doping by Dimers of Benzimidazoline Radicals, *Adv. Mater.*, 2014, **26**, 4268–4272.
8 X. Lin, B. Wegner, K. M. Lee, M. A. Fusella, F. Zhang, K. Moudgil, B. P. Rand, S. Barlow, S. R. Marder, N. Koch and A. Kahn, Beating the thermodynamic limit with photo-activation of n-doping in organic semiconductors, *Nat. Mater.*, 2017, **16**, 1209–1215.
9 E. E. Perry, C.-Y. Chiu, K. Moudgil, R. A. Schlitz, C. J. Takacs, K. A. O'Hara, J. G. Labram, A. M. Glaudell, J. B. Sherman, S. Barlow, C. J. Hawker, S. R. Marder and M. L. Chabinyc, High Conductivity in a Nonplanar *n*-Doped Ambipolar Semiconducting Polymer, *Chem. Mater.*, 2017, **29**, 9742–9750.
10 Y. Qi, S. K. Mohapatra, S. Bok Kim, S. Barlow, S. R. Marder and A. Kahn, Solution doping of organic semiconductors using air-stable n-dopants, *Appl. Phys. Lett.*, 2012, **100**, 083305–4.
11 Y. Zhou, C. Fuentes-Hernandez, J. Shim, J. Meyer, A. J. Giordano, H. Li, P. Winget, T. Papadopoulos, H. Cheun, J. Kim, M. Fenoll, A. Dindar, W. Haske, E. Najafabadi, T. M. Khan, H. Sojoudi, S. Barlow, S. Graham, J.-L. Bredas, S. R. Marder, A. Kahn and B. Kippelen, A Universal Method to Produce Low-Work Function Electrodes for Organic Electronics, *Science*, 2012, **336**, 327–332.
12 B. Russ, M. J. Robb, B. C. Popere, E. E. Perry, C.-K. Mai, S. L. Fronk, S. N. Patel, T. E. Mates, G. C. Bazan, J. J. Urban, M. L. Chabinyc, C. J. Hawker and R. A. Segalman, Tethered tertiary amines as solid-state n-type dopants for solution-processable organic semiconductors, *Chem. Sci.*, 2016, **7**, 1914–1919.
13 S. B. Schmidt, T. Biskup, X. Jiao, C. R. McNeill and M. Sommer, Controlling intermolecular redox-doping of naphthalene diimides, *J. Mater. Chem. C*, 2019, **7**, 4466–4474.
14 S. Fabiano, S. Braun, X. Liu, E. Weverberghs, P. Gerbaux, M. Fahlman, M. Berggren and X. Crispin, Poly(ethylene imine) Impurities Induce n-doping Reaction in Organic (Semi)Conductors, *Adv. Mater.*, 2014, **26**, 6000–6006.
15 A. Cabrera-Espinoza, S. Collavini and J. L. Delgado, Doping strategies of organic n-type materials in perovskite solar cells: a chemical perspective, *Sustain*, *Energy Fuels*, 2020, **4**, 3264–3281.
16 J. Panidi, J. Kainth, A. F. Paterson, S. Wang, L. Tsetseris, A. Emwas, M. A. McLachlan, M. Heeney and T. D. Anthopoulos, Introducing a Nonvolatile N-Type Dopant Drastically Improves Electron Transport in Polymer and Small-Molecule Organic Transistors, *Adv. Funct. Mater.*, 2019, **29**, 1902784.
17 A. Skiebe, A. Hirsch, H. Klos and B. Gotschy, [DBU]C60. Spin pairing in a fullerene salt, *Chem. Phys. Lett.*, 1994, **220**, 138–140.
18 H. Klos, I. Rystau, W. Schütz, B. Gotschy, A. Skiebe and A. Hirsch, Doping of C60 with tertiary amines: TDAE, DBU, DBN. A comparative study, *Chem. Phys. Lett.*, 1994, **224**, 333–337.
19 L. Hu, T. Liu, J. Duan, X. Ma, C. Ge, Y. Jiang, F. Qin, S. Xiong, F. Jiang, B. Hu, X. Gao, Y. Yi and Y. Zhou, An Amidine-Type n-Dopant for Solution-Processed Field-Effect Transistors and Perovskite Solar Cells, *Adv. Funct. Mater.*, 2017, **27**, 1703254.
20 R. Ge, F. Qin, L. Hu, S. Xiong and Y. Zhou, High fill factor over 82% enabled by a biguanide doping electron transporting layer in planar perovskite solar cells, *Front. Optoelectron.*, 2018, **11**, 360–366.
21 R. Pratt, B. Lohmeijer, D. Long, R. Waymouth and J. Hedrick, *J. Am. Chem. Soc.*, 2006, **128**, 4556–4557.
22 X. Fu and C.-H. Tan, Mechanistic considerations of guanidine-catalyzed reactions, *Chem. Commun.*, 2011, **47**, 8210.
23 Z. Tang, J. Wang, A. Melianas, Y. Wu, R. Kroon, W. Li, W. Ma, M. R. Andersson, Z. Ma, W. Cai, W. Tress and O. Inganäs, Relating open-circuit voltage losses to the active layer morphology and contact selectivity in organic solar cells, *J. Mater. Chem. A*, 2018, **6**, 12574–12581.
24 R. A. Schlitz, F. G. Brunetti, A. M. Glaudell, P. L. Miller, M. A. Brady, C. J. Takacs, C. J. Hawker and M. L. Chabinyc, Solubility-Limited Extrinsic n-Type Doping of a High Electron Mobility Polymer for Thermoelectric Applications, *Adv. Mater.*, 2014, **26**, 2825–2830.
25 P. Gund, Guanidine, trimethylenemethane, and 'Y-delocalization.' Can acyclic compounds have 'aromatic' stability?, *J. Chem. Educ.*, 1972, **49**, 100.
26 A. Dworkin, R. Naumann, C. Seigfred, J. M. Karty and Y. Mo, Y-Aromaticity: Why Is the Trimethylenemethane Dication More Stable than the Butadienyl Dication?, *J. Org. Chem.*, 2005, **70**, 7605–7616.
27 C. Burkholder, W. Dolbier and M. Medebielle, *J. Org. Chem.*, 1998, **63**, 5385–5394.
28 S. Wang, H. Sun, U. Ail, M. Vagin, P. O. Å. Persson, J. W. Andreasen, W. Thiel, M. Berggren, X. Crispin, D. Fazzi and S. Fabiano, Thermoelectric Properties of Solution-Processed n-Doped Ladder-Type Conducting Polymers, *Adv. Mater.*, 2016, **28**, 10764–10771.
29 G. Yu, J. Gao, J. C. Hummelen, F. Wudl and A. J. Heeger, Polymer Photovoltaic Cells: Enhanced Efficiencies *via* a Network of Internal Donor-Acceptor Heterojunctions, *Science*, 1995, **270**, 1789–1791.
30 M. Schwarze, C. Gaul, R. Scholz, F. Bussolotti, A. Hofacker, K. S. Schellhammer, B. Nell, B. D. Naab, Z. Bao, D. Spoltore,

Published on 27 juli 2020. Downloaded on 03.08.2025 1:40:23.

K. Vandewal, J. Widmer, S. Kera, N. Ueno, F. Ortmann and K. Leo, Molecular parameters responsible for thermally activated transport in doped organic semiconductors, *Nat. Mater.*, 2019, **18**, 242–248.

31 S. Rossbauer, C. Müller and T. D. Anthopoulos, Comparative Study of the N-Type Doping Efficiency in Solution-processed Fullerenes and Fullerene Derivatives, *Adv. Funct. Mater.*, 2014, **24**, 7116–7124.

32 Y. Park, C. Fuentes-Hernandez, X. Jia, F. A. Larrain, J. Zhang, S. R. Marder and B. Kippelen, Measurements of the field-effect electron mobility of the acceptor ITIC, *Org. Electron.*, 2018, **58**, 290–293.

33 Y. Guo, W. Sato, K. Inoue, W. Zhang, G. Yu and E. Nakamura, n-Type doping for efficient polymeric electron-transporting layers in perovskite solar cells, *J. Mater. Chem. A*, 2016, **4**, 18852–18856.

34 J. Zhou, J. Hou, X. Tao, X. Meng and S. Yang, Solution-processed electron transport layer of n-doped fullerene for efficient and stable all carbon based perovskite solar cells, *J. Mater. Chem. A*, 2019, **7**, 7710–7716.

35 J. Wang, W. Fu, S. Jariwala, I. Sinha, A. K.-Y. Jen and D. S. Ginger, Reducing Surface Recombination Velocities at the Electrical Contacts Will Improve Perovskite Photovoltaics, *ACS Energy Lett.*, 2019, **4**, 222–227.

36 N. K. Noel, S. N. Habisreutinger, A. Pellaroque, F. Pulvirenti, B. Wenger, F. Zhang, Y.-H. Lin, O. G. Reid, J. Leisen, Y. Zhang, S. Barlow, S. R. Marder, A. Kahn, H. J. Snaith, C. B. Arnold and B. P. Rand, Interfacial charge-transfer doping of metal halide perovskites for high performance photovoltaics, *Energy Environ. Sci.*, 2019, **12**, 3063–3073.

37 S. Shao, J. Liu, H.-H. Fang, L. Qiu, G. H. ten Brink, J. C. Hummelen, L. J. A. Koster and M. A. Loi, Efficient Perovskite Solar Cells over a Broad Temperature Window: The Role of the Charge Carrier Extraction, *Adv. Energy Mater.*, 2017, **7**, 1701305.

38 S. van Reenen, S. Kouijzer, R. A. J. Janssen, M. M. Wienk and M. Kemerink, Origin of Work Function Modification by Ionic and Amine-Based Interface Layers, *Adv. Mater. Interfaces*, 2014, **1**, 1400189.

39 H. Zhou, Q. Chen, G. Li, S. Luo, T.-B. Song, H.-S. Duan, Z. Hong, J. You, Y. Liu and Y. Yang, Interface engineering of highly efficient perovskite solar cells, *Science*, 2014, **345**, 542–546.

40 J. You, Y. (Michael) Yang, Z. Hong, T.-B. Song, L. Meng, Y. Liu, C. Jiang, H. Zhou, W.-H. Chang, G. Li and Y. Yang, Moisture assisted perovskite film growth for high performance solar cells, *Appl. Phys. Lett.*, 2014, **105**, 183902.

41 C. Sun, Z. Wu, H.-L. Yip, H. Zhang, X.-F. Jiang, Q. Xue, Z. Hu, Z. Hu, Y. Shen, M. Wang, F. Huang and Y. Cao, Amino-Functionalized Conjugated Polymer as an Efficient Electron Transport Layer for High-Performance Planar-Heterojunction Perovskite Solar Cells, *Adv. Energy Mater.*, 2016, **6**, 1501534.

42 E. E. Perry, J. G. Labram, N. R. Venkatesan, H. Nakayama and M. L. Chabinyc, N-Type Surface Doping of $MAPbI_3$ via Charge Transfer from Small Molecules, *Adv. Electron. Mater.*, 2018, **4**, 1800087.

43 P. J. Bailey and S. Pace, The coordination chemistry of guanidines and guanidinates, *Coord. Chem. Rev.*, 2001, **214**, 91–141.

44 F. T. Edelmann, *Advances in Organometallic Chemistry*, Elsevier, 2013, vol. 61, pp. 55–374.

45 Z.-Z. Yang, Y.-N. Zhao and L.-N. He, CO_2 chemistry: task-specific ionic liquids for CO_2 capture/activation and subsequent conversion, *RSC Adv.*, 2011, **1**, 545.

46 C. Villiers, J.-P. Dognon, R. Pollet, P. Thuéry and M. Ephritikhine, An Isolated CO_2 Adduct of a Nitrogen Base: Crystal and Electronic Structures, *Angew. Chem., Int. Ed.*, 2010, **49**, 3465–3468.

47 C. M. Geiselhart, C. W. Schmitt, P. Jöckle, H. Mutlu and C. Barner-Kowollik, A Guanidine-Based Superbase as Efficient Chemiluminescence Booster, *Sci. Rep.*, 2019, **9**, 14519.

48 N. Watanabe, A. Wakatsuki, H. K. Ijuin, Y. Kabe and M. Matsumoto, Organic superbase-induced chemiluminescent decomposition of a hydroxyaryl-substituted dioxetane: Unique effect of a bifunctional guanidine base on the chemiluminescence profile of a bicyclic dioxetane bearing a 4-(benzoxazol-2-yl)-3,5-dihydroxyphenyl moiety, *Tetrahedron Lett.*, 2018, **59**, 971–977.

 This journal is © The Royal Society of Chemistry and the Chinese Chemical Society 2020